SAND2022-12739C

Reverse Breakdown Time of Wide Bandgap Diodes

Jack Flicker
Power Electronics and Energy Conversion Systems
Sandia National Laboratories
Albuquerque, NM USA
jdflick@sandia.gov

Emily Schrock
Directed Energy Missions
Sandia National Laboratories
Albuquerque, NM USA
eschroc@sandia.gov

Robert Kaplar
Semiconductor Material and Device Sciences
Sandia National Laboratories
Albuquerque, NM USA
rjkapla@sandia.gov

***Abstract*—In order to evaluate the time evolution of avalanche breakdown in wide and ultra-wide bandgap devices, we have developed a cable pulser experimental setup that can evaluate the time-evolution of the terminating impedance for a semiconductor device with a time resolution of 130 ps. We have utilized this pulser setup to evaluate the time-to-breakdown of vertical Gallium Nitride and Silicon Carbide diodes for possible use as protection elements in the electrical grid against fast transient voltage pulses (such as those induced by an electromagnetic pulse event). We have found that the Gallium Nitride device demonstrated faster dynamics compared to the Silicon Carbide device, achieving 90% conduction within 1.37 ns compared to the SiC device response time of 2.98 ns. While the Gallium Nitride device did not demonstrate significant dependence of breakdown time with applied voltage, the Silicon Carbide device breakdown time was strongly dependent on applied voltage, ranging from a value of 2.97 ns at 1.33 kV to 0.78 ns at 2.6 kV. The fast response time (< 5 ns) of both the Gallium Nitride and Silicon Carbide devices indicate that both materials systems could meet the stringent response time requirements and may be appropriate for implementation as protection elements against electromagnetic pulse transients.**

Keywords—impact ionization, avalanche breakdown, EMP protection, SiC, GaN, WBG, UWBG

I. Introduction

One of the primary advantages of wide and ultra-wide bandgap (U/WBG) devices is their increased breakdown electric field compared to conventional semiconductor materials [1]. In vertical devices, this increased voltage hold-off allows for thinner active regions, which results in lower cost and faster switching dynamics. The importance of breakdown electric field for semiconductor device can be seen in typical figures of merit (FOMs) that are used to compare performance across materials systems. For example, the Baliga Figure of Merit (BFOM) [2] scales as the cube of the breakdown electric field, the Huang FOM (HCAFOM) [3] scales as the breakdown electric field squared, and the Johnson FOM (JFOM) [4] scale linearly with the breakdown electric field. Although it is important to note that these FOMs are approximations that do not consider the dependence of breakdown electric field on doping, temperature, and a variety of other more complicated factors [5], they are still utilized extensively to compare the appropriateness of possible materials systems in a given application.

The intrinsic process which limits voltage hold-off in semiconductor devices is impact ionization or avalanche breakdown [6]. Due to the importance of understanding avalanche breakdown, significant effort has been expended in the literature on elucidating the process using a variety of analytical and phenomenological models [7-10] and measuring breakdown electric field and/or impact ionization coefficients for U/WBG materials [5]. These measurements typically are carried out under static or pseudo-static conditions to evaluate the magnitude of breakdown electric field.

U/WBG devices with high static voltage hold-off and fast carrier dynamics are ideal for utilization as protection elements against high-voltage, fast transient wavefronts, for example for high voltage electromagnetic pulse (EMP) protection of the electrical grid. The fastest protection elements on the grid are typically metal oxide varistors (MOVs) composed of packed granular power columns of zinc oxide (ZnO) powder that are designed as lightning surge arresters (LSAs) and tested to ~1 μs response times [11].

EMP is a complicated multi-step process that is typically split into three regimes; a fast risetime wave (<10 ns) known as E1, a medium risetime wave (~1 μs) known as E2, and a slow wave (~minutes to hours) known as E3 [12]. While conventional LSAs may offer protection against E2 dynamics, modeling/testing has shown that they are too slow to arrest the E1 component of the EMP wavefront [13, 14] with charge-migration rates at grain boundary interfaces limiting response times to tens to hundreds of nanoseconds [15, 16].

Due to their small size, high breakdown electric field, and fast dynamic response U/WBG diodes may be ideal protection devices on the electrical grid to protect against E1-type transients. These diodes can be placed in the power system to provide coordinated protection at fast time scales (~ns) before traditional LSAs can actuate (~1 μs). These diodes would utilize avalanche breakdown, so that any applied voltage greater than the breakdown voltage (V_{br}) would induce conduction and shunt current to ground. The highly non-linear conduction would quickly clamp voltages at the diode breakdown voltage until traditional LSAs can react (~1 μs).

Utilization of U/WBG diodes as protection devices depends not only on the static breakdown electric field, but also on the dynamics of the avalanche process, which determines the timescale of voltage clamping. While significant effort has been made to understand the static or pseudo-static characteristics of the avalanche mechanism in U/WBG device, much less effort has been made to evaluate the dynamics of this process. In this work, we describe a test setup to evaluate

The authors are thankful for the support from ULTRA, an Energy Frontier Research Center funded by the U.S. Department of Energy (DOE), Office of Science, Basic Energy Sciences (BES), under Award No. DE-SC0021230. The work is also supported, in part, by ARPA-E's OPEN+ Kilovolt Devices Cohort directed by Dr.Isik Kiz

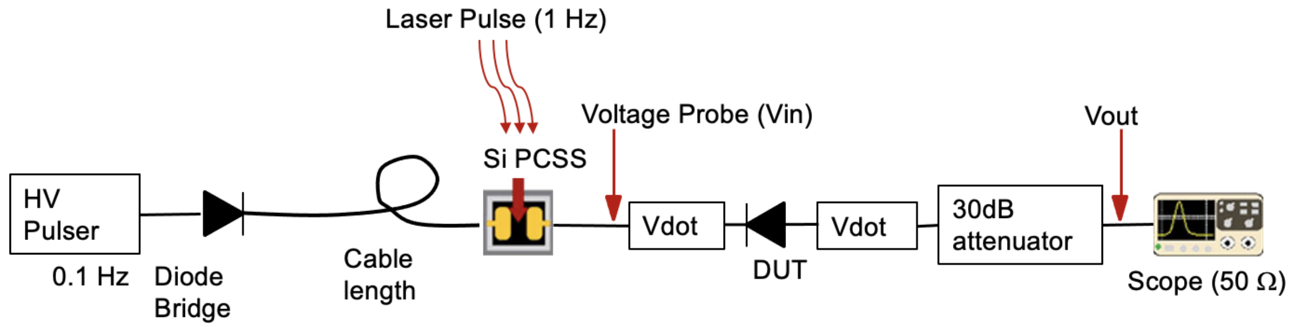

Figure 1: Experimental test setup to measure time-based reverse breakdown characteristics of a device under test

the time dynamics of diode avalanche breakdown and describe results on vertical SiC Schottky and GaN pin diodes.

II. Reverse BreakdownTesting Setup

In previous work [17] we have described a novel pulser measurement capability to evaluate ultra-fast reverse recovery time of WBG diodes based on previous work on light emitting diodes [18]. Briefly, this reverse recovery measurement is a subset of time domain reflectometry (TDR) measurements where an input pulse waveform interacts with a reflected waveform from the cable termination interface (i.e., the load). The nature of this interaction can give information regarding both the time-of-flight and load impedance based on the reflection coefficient, Γ. An open circuit results in Γ=1 with constructive interference between the incident and reflected wave, resulting in a measured voltage doubling of the incident wave. A short circuit results in Γ=−1 with destructive interference with the incident wave. A matched impedance (typically 50 Ω) results in Γ=0 with no reflected wave. By evaluating the evolution of the incident waveform over time (and thus the value of $\Gamma(t)$), it is possible to track the evolution of load impedance over time with very high time resolution.

This pulser setup was previously utilized to measure the reverse recovery time of vertical Gallium Nitride (v-GaN) diodes with resolution ~100ps. To measure reverse recovery, the device under test (DUT) was forward biased by a small voltage in the conducting regime ($\Gamma \approx$-1). A high voltage incident pulse was applied to force the diode into a blocking state ($\Gamma \approx 1$). Capacitive (V-dot) probes [19] were utilized to evaluate the time-evolution of the incident pulse to extract the evolution of Γ over time.

To change the measurement from the previous time-based reverse recovery measurements (conduction-to-blocking) to time-based reverse breakdown (blocking-to-breakdown conduction), this pulser experimental setup has been slightly altered. Figure 1 shows a diagram schematic of the experimental setup.

The main components of the system are a pulse generating circuit, the device under test, and diagnostic components. The pulse generating system is composed of a high voltage pulse charging circuit (capable of pulse voltages up to 3 kV), a diode bridge and cable length for charge storage (to give control over pulse length), a Silicon (Si) photoconductive semiconductor switch (PCSS) which controls voltage application to the DUT, and a triggering laser. Details of these components can be found in [17].

The DUT is electrically connected to a copper strip line on a standard printed circuit board (PCB) FR4 substrate. This PCB is sandwiched between two aluminum outer conductor pieces to form a two-port, high-bandwidth, 50 Ω enclosure that is connected to the cable pulser via N-type connectors. Since the diode does not need to be biased prior to measuring (as in [17]), instead of terminating with a current viewing resistor (CVR) and biasing voltage, the cable pulser is terminated with an impedance-matched (50 Ω) 4 GHz oscilloscope (Tektronix TDS7404). Diagnostic voltage probes are present both before and after the DUT, allowing evaluation of both the reflected and conducted pulses on either side of the DUT.

In this setup, the pulse generation circuit generates a fast rise-time reverse-biasing pulse which is applied to the diode with a 130 ps rise-time via the transmission line (10-90% threshold under open circuit). When the pulse reaches the diode being tested, it forces the diode from a non-biased blocking state to a reverse-bias blocking state. This reverse bias blocking state has a very high impedance, and the pulser will be terminated by the DUT with a reflection coefficient that is nearly that of an open circuit (i.e., $\Gamma \approx 1$).

If the voltage pulse is large enough to initiate avalanche breakdown, the diode will enter a reverse bias conducting state. During this transition, the impedance of the diode changes from high-impedance to low-impedance, thus causing the diode to exhibit a dynamic reflection coefficient. In this case, initially the pulser will be terminated by the high-impedance DUT ($\Gamma \approx 1$), but as the system evolves in time and the diode impedance decreases, the pulser will be terminated by the impedance-matched oscilloscope (i.e., $\Gamma \approx 0$). This results in a voltage collapse on the input to halve the applied voltage, while simultaneously a voltage rise on the DUT output indicates DUT conduction.

The response time of two types of power semiconductor diodes were evaluated: a vertical GaN device from Avogy Inc. and a vertical SiC device from On Semiconductor (OnSemi).

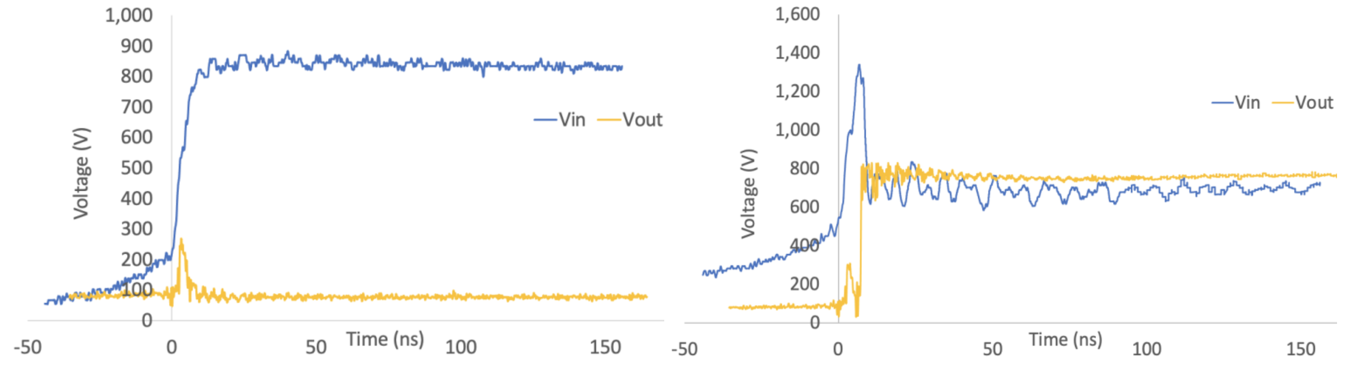

Figure 2: (Left) Input (blue) and output (yellow) voltages for SiC DUT in blocking mode ($V_{applied} < V_{br}$). (Right). Input (blue) and output (yellow) voltages for SiC DUT in reverse breakdown mode ($V_{applied} > V_{br}$).

The v-GaN devices from Avogy (AVD05120 series) are a true vertical structure, grown on conducting native GaN substrates. These PiN diodes consist of an n^+ wafer, an n^- drift region, and a p^+ anode as well as the required edge termination structures [20-22]. The diodes are rated for 1200 V and 100 A (pulsed).

The SiC devices from OnSemi (NGTD17R120F2) [23] are Schottky diodes nominally designed for flyback protection of insulated gate bipolar transistor (IGBT) switches. The diodes are rated for 1200 V and 35 A (DC).

III. Results and Discussion

Figure 2 shows the results for a voltage pulse applied to a SiC diode for an applied voltage below breakdown (left) and just above breakdown (right). The voltage profile is reconstructed through integration of the signal of the V-dot probe located before the DUT (blue) and just after the DUT (yellow).

At voltages below breakdown (Figure 2, left), the PCSS is triggered via the triggering laser at t = 0. Prior to triggering at t = 0, there is a slight voltage rise at the input of the diode (blue) due to leakage through the Si PCSS. The actuation of the PCSS at t=0 applies a voltage step to the diode of 850 V. The applied voltage is not at a true steady-state during hold-off but is slowly decreasing (~ms) due to charge dissipation in the diode bridge and cable of the pulser. However, in the regime of interest (<< 1 µs), the voltage can be approximated by a step function.

The V-dot measurement on the output of the diode is shown in yellow. This trace shows a transient voltage pulse during the voltage step with a duration of ~4 ns. This transient voltage measurement indicates displacement current due to charging the junction capacitance of the diode [24] as voltage is applied to the diode.

At voltages above breakdown (Figure 2, right), the characteristic input (blue) and output (yellow) voltage traces look significantly different. When the PCSS is triggered (t = 0), the input voltage (blue trace) rises to a maximum value of 1.3kV and then collapses down to a voltage of ~750 V, approximately ½ of the full applied voltage. This voltage collapse from full voltage to ½ of the full applied voltage indicates that there is no longer voltage doubling ($\Gamma = 1$) and that the device is now conducting with the pulser being terminated by the impedance-matched oscilloscope ($\Gamma = 0$).

Simultaneously, as the voltage at the input of the diode collapses, there is an increase in voltage measured at the output of the diode (yellow) to the applied voltage. This voltage increase on the output of the diode to approximately the same magnitude of the total voltage indicates the diode is in conduction with an intrinsic resistance that is much smaller than the pulser termination (i.e., 50 Ω).

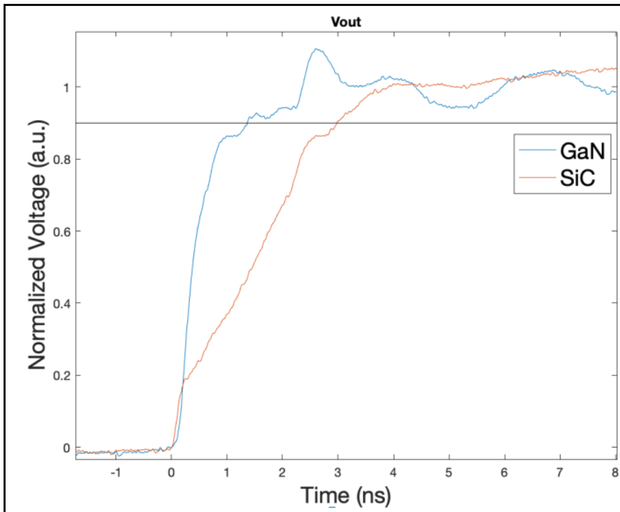

Figure 3: Output voltage of SiC (red) and GaN (blue) devices at breakdown.

To define the value the output voltage signal was approaching and the 90% threshold determining the end of the breakdown transients more accurately, the output voltage was normalized to the measured steady-state output voltage. For this normalized voltage measurement, a value of 0 indicates a fully blocking state while a value of 1 indicates fully conducting state. Figure 3 shows the normalized results for the GaN and SiC diodes at an applied voltage just above V_{br} at an applied voltage of 1.22 and 1.33 kV, respectively. Both devices cross the 90% threshold within 3 ns of the PCSS trigger pulse. The GaN device achieved breakdown significantly faster, with the 90% threshold being reached at 1.37 ns compared to 2.98 ns for SiC. Both devices respond within the nanosecond regime needed for protection elements. However, due to the difference in device materials stack, type, and footprint, it is difficult to make accurate apples-to-apples comparisons about the applicability of both materials systems.

Response times of both the GaN and SiC devices were measured at applied voltages ranging from just above V_{br} to $2*V_{br}$. The GaN device showed little dependence on the applied voltage. However, the SiC response time reduced significantly with increased voltage (TABLE I) from a value of 2.97 ns at 1.33 kV to 0.78 ns at 2.6 kV (a 3.8x reduction in response time). The applied voltage significantly increases the slope of the breakdown transient (Figure 4). The root cause of this and why this effect is not seen as dramatically in GaN is still under investigation to determine whether this effect is due to the intrinsic breakdown mechanisms within SiC, dynamics in the Schottky barrier, or the junction capacitance of the device.

TABLE I. SIC DIODE 90% RESPONSE TIME UNDER DIFFERENT APPLIED VOLTAGE

Applied Voltage (kV)	*90% threshold time (ns)*
1.33	2.98
1.7	2.42
1.8	2.17
2.35	0.82
2.5	0.90
2.6	0.78

IV. Conclusions

In this work, we have introduced a variation of a previously developed experimental pulser technique originally used to measure the fast reverse recovery time of WBG diodes with resolution of 130 ps. This variation evaluates the dynamic reflection coefficient (Γ) of the terminating DUT under applied reverse bias voltage pulses. When voltage pulses above the breakdown of the device are applied, the time evolution of device avalanche breakdown can be monitored from fully blocking through fully conducting.

This experimental technique was used to evaluate two 1200 V vertical WBG devices, a v-GaN pin diode from Avogy, Inc. and a SiC Schottky diode from OnSemi. At an applied voltage

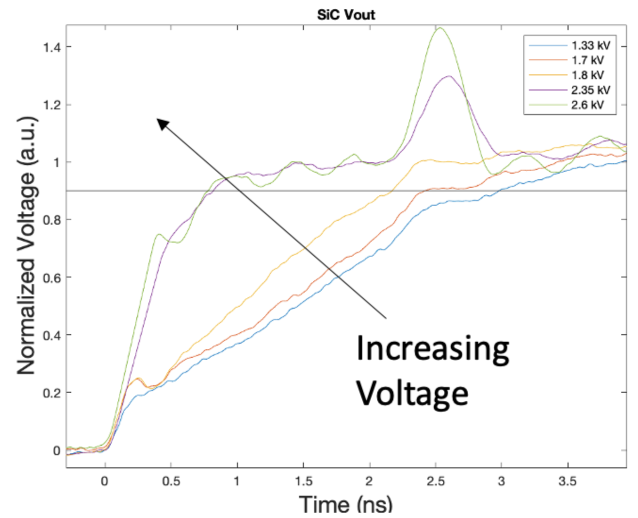

Figure 4: Avalanche response of SiC diode to applied voltages from 1.33 kV to 2.6 kV.

just above breakdown, both devices achieved the 90% conduction threshold within 3 ns. The v-GaN device demonstrated faster dynamics compared to the SiC device. The v-GaN device achieved 90% conduction within 1.37 ns compared to the SiC device response time of 2.98 ns. The v-GaN device did not demonstrate significant dependence of breakdown time with applied voltage. However, the SiC device breakdown time was strongly dependent on applied voltage, ranging from a value of 2.97 ns at 1.33 kV to 0.78 ns at 2.6 kV.

The high voltage hold-off of WBG diodes coupled with the repeatable, fast dynamics of avalanche breakdown make them appealing as high-speed protection devices in high voltage systems. An example of this is the EMP E1 transient mitigation on the electrical power grid. As the risetime of an E1 pulse is typically <10 ns, devices must exhibit response times faster than this to be considered as a protection element. The work presented here has demonstrated that both GaN and SiC diodes can meet these stringent response time requirements and may be appropriate for implementation as protection elements against E1 transients.

Acknowledgment

Sandia National Laboratories is a multimission laboratory managed and operated by National Technology & Engineering Solutions of Sandia, LLC, a wholly owned subsidiary of Honeywell International Inc., for the U.S. Department of Energy's National Nuclear Security Administration under contract DE-NA0003525.

References

[1] J. Y. Tsao *et al.*, "Ultrawide-Bandgap Semiconductors: Research Opportunities and Challenges," *Advanced Electronic Materials,* vol. 4, no. 1, pp. 1600501-n/a, 2018, Art no. 1600501, doi: 10.1002/aelm.201600501.

[2] K. Shenai, R. S. Scott, and B. J. Baliga, "Optimum semiconductors for high-power electronics," *IEEE Trans. Electr. Dev.,* vol. 36, no. 9, pp. 1811-1823, 1989.

[3] A. Q. Huang, "New unipolar switching power device figures of merit," *IEEE Electron Device Letters,* vol. 25, no. 5, pp. 298-301, 2004, doi: 10.1109/LED.2004.826533.
[4] E. O. Johnson, "Physical limitations on frequency and power parameters of transistors," in *Semiconductor Devices: Pioneering Papers*: World Scientific, 1991, pp. 295-302.
[5] O. Slobodyan *et al.*, "Analysis of the dependence of electric field on semiconductor bandgap," *Journal of Materials Research,* pp. 1-17, 2022.
[6] S. M. Sze and K. K. Ng, *Physics of semiconductor devices*. John wiley & sons, 2006.
[7] B. Ridley, "Lucky-drift mechanism for impact ionisation in semiconductors," *Journal of Physics C: Solid State Physics,* vol. 16, no. 17, p. 3373, 1983.
[8] P. Wolff, "Theory of electron multiplication in silicon and germanium," *Physical Review,* vol. 95, no. 6, p. 1415, 1954.
[9] W. Shockley, "Problems related to p-n junctions in silicon," *Solid-State Electronics,* vol. 2, no. 1, pp. 35-67, 1961/01/01/ 1961, doi: https://doi.org/10.1016/0038-1101(61)90054-5.
[10] A. G. Chynoweth, "Ionization rates for electrons and holes in silicon," *physical review,* vol. 109, no. 5, p. 1537, 1958.
[11] *IEEE Standard for Metal-Oxide Surge Arresters for AC Power Circuits, C62.11-2012*, IEEE Power and Energy Society, New York, NY, 2012.
[12] E. Savage, J. Gilbert, and W. Radasky, "The early-time (E1) high-altitude electromagnetic pulse (HEMP) and its impact on the US power grid," *Report Meta,* 2010.
[13] A. G. Tarditi *et al.*, "High Voltage Modeling and Testing of Transformer, Line Interface Devices, and Bulk System Components Under Electromagnetic Pulse, Geomagnetic Disturbance, and other Abnormal Transients," Oak Ridge National Lab.(ORNL), Oak Ridge, TN (United States), 2019.
[14] T. Bowman, M. Halligan, and R. Llanes, "High-Frequency Metal-Oxide Varistor Modeling Response to Early-time Electromagnetic Pulses," in *2020 IEEE International Symposium on Electromagnetic Compatibility & Signal/Power Integrity (EMCSI)*, 2020: IEEE, pp. 466-471.
[15] A. Varpula, "Modeling of transient electrical characteristics for granular semiconductors," *Journal of Applied Physics,* vol. 108, no. 3, p. 034511, 2010.
[16] G. Xie, M. Wu, and W. Shi, "Boundary breakdown time of ZnO varistors under nanosecond pulse current," *AIP Advances,* vol. 9, no. 4, p. 045032, 2019.
[17] Daniel L. Mauch *et al.*, "Ultra-Fast Reverse Recovery Measurement for Wide-Bandgap Diodes," 2016 (*Submitted IEEE Transactions on Power Electronics).*
[18] R. H. Dean and C. J. Nuese, "A refined step-recovery technique for measuring minority carrier lifetimes and related parameters in asymmetric pn junction diodes," *IEEE Trans. Electr. Dev.,* vol. 18, no. 3, pp. 151-158, 1971.
[19] H. Bluhm, "Power Systems," 2006.
[20] C. Matthews *et al.*, "Switching characterization of vertical GaN PiN diodes," in *2016 IEEE 4th Workshop on Wide Bandgap Power Devices and Applications (WiPDA)*, 2016: IEEE, pp. 135-138.
[21] I. C. Kizilyalli, A. P. Edwards, O. Aktas, T. Prunty, and D. Bour, "Vertical Power p-n Diodes Based on Bulk GaN," *IEEE Trans. Electr. Dev.,* vol. 62, no. 2, pp. 414-422, 2015, doi: 10.1109/TED.2014.2360861.
[22] I. C. Kizilyalli, A. P. Edwards, H. Nie, D. Disney, and D. Bour, "High Voltage Vertical GaN p-n Diodes With Avalanche Capability," *IEEE Trans. Electr. Dev.,* vol. 60, no. 10, pp. 3067-3070, 2013, doi: 10.1109/TED.2013.2266664.
[23] On Semiconductor, "NGTD17R120F2: Fast Switching Rectifier Die," March 2016. Available: https://www.onsemi.com/pdf/datasheet/ngtd17r120f2wp-d.pdf Accessed:Sept 8, 2022.
[24] T. Funaki, T. Kimoto, and T. Hikihara, "Evaluation of high frequency switching capability of SiC Schottky barrier diode, based on junction capacitance model," *IEEE transactions on power electronics,* vol. 23, no. 5, pp. 2602-2611, 2008.